Effect of Resolidification Conditions on $Bi_2Sr_2CaCu_2O_x$/Ag/AgMg Coil Performance

Xiaotao T. Liu, William T. Nachtrab, Terry Wong, and Justin Schwartz, *Fellow, IEEE*

***Abstract*—The performance of $Bi_2Sr_2CaCu_2O_x$ (Bi2212) wires is very sensitive to the heat treatment conditions, and in particular to the conditions immediately after partial-melting. In this paper, the effect of solidification conditions on Bi2212/Ag/AgMg coil performance is investigated using a split melt process. After partial melting, Bi2212 is first cooled with a relatively fast cooling rate, 10°C/hr, for a short time until reaching "T_1" and subsequently by a slower cooling rate, 2.5°C/hr, for a much longer period of time. Here we study the effects of varying T_1. With decreasing T_1, the overall effective cooling rate during resolidification, particularly the initial stage of resolidification, is increased. As a result, the Bi2212 grain size and the bridges between filaments are inhibited. For short witness samples heat treated with the coils, the transport current and the connectivity decrease with decreasing T_1. A similar tendency is observed in coils, however the coils also show inhomogeneous performance within the conductor. In coils the end sections have higher transport critical current and better connectivity than the middle sections. With decreasing T_1 the difference between end sections and middle sections also decreases. Microanalysis shows that with the insulation on the conductor (both witness samples and short samples cut from coil sections) during heat treatment, increased copper-free phases are found in the Bi2212 filaments as compared to the witness samples heat treated without insulation. In short samples cut from coils, microanalysis also shows an increase in the number of outer filaments that are lost. EDS analysis indicates that Ag and Cu react with the insulation fiber. The Cu diffuses through the Ag sheath and reacts with the insulation fiber, leading to Cu deficiency in the filaments.**

***Index Terms*—Bi2212/Ag round wire, high-temperature superconductors, superconducting magnets.**

I. Introduction

THE $Bi_2Sr_2CaCu_2O_x$ (Bi2212) high temperature superconductor, in the form of a multifilamentary round wire, has excellent electrical performance in high magnetic field at 4.2 K, which indicates that Bi2212 has great potential for use in high-field superconducting magnets generating magnetic fields greater than 21 T where low temperature superconductors reach a fundamental limit due to low B_{c2} [1], [2]. In magnet applications, solenoid winding using round or rectangular wires is advantageous over tape conductors because of higher packing fraction and ease of layer-to-layer transitions. Bi2212 is the only high temperature superconductor which can be fabricated into round wire with high J_e and no electromagnetic anisotropy. For these reasons, and the relative ease of cabling round wire, Bi2212 round wire is one of the most promising candidates for a high field insert magnets, NMR magnets and high energy physics magnets [3], [4].

Traditionally there are two approaches to magnet manufacturing, react-and-wind (R&W) and wind-and-react (W&R). For brittle materials like Bi2212, W&R is typically preferred so as to avoid bending strain after heat treatment [2].

Partial melt-processing is one of the most widely used techniques for producing highly textured Bi2212 wires and tapes. It consists of melting the material above its peritectic temperature, rapid cooling from peak temperature to a temperature (T_1) above $T_{solidus}$, slow cooling to a temperature below $T_{solidus}$, and isothermal annealing [5], [6]. Split melt processing is a two-step process developed in conjunction with the react-wind-sinter approach to magnet manufacturing. During split melt processing, the partial melt-processing is interrupted during the slow cooling step and split into two heat treatments [5], [7], [8]. Here, the split melt process is used to study the effects of varying the time above $T_{solidus}$ by varying T_1 and determining the effects on the transport critical current, magnetization and microstructure Bi2212 coils.

II. Experimental Details

In this study, multifilamentary $Bi_2Sr_2CaCu_2O_x$/AgMg wire is manufactured with a single-restack design as shown in Fig. 1(a). After final deformation, the wire diameter is 0.787 mm with a 37% fill factor and a 15 μm average filament diameter. The wire is insulated with braided mullite ($70\%Al_2O_3/30\%SiO_2$) and wound on a 35 mm diameter inconel tube. Each coil uses 1.2 m of conductor. A typical single-layer coil is seen in Fig. 1(b) (before heat treatment) and Fig. 1(c) (after heat treatment). The heat treatment profile used is shown in Fig. 2. The profile consists of two heat treatments, a melting and solidification process and an annealing process, separated by a cooling to room temperature. The temperature-time profile for the first heat treatment is a ramp from room temperature to 821°C at 160°C/h, hold for 2 h, heat to the peak temperature (T_p, 884°C) at 50°C/h, hold for 0.2 h, cool at 10°C/h to T_1, cool at 2.5°C/h to 833°C, and cool at 160°C/h to room temperature. During the first heat treatment, T_1 was varied from 833°C to 877°C and the sintering time is adjusted to keep the solidification time constant (18.3 h from the end of T_p to the beginning of cooling to room temperature).

Manuscript received August 27, 2008. First published June 05, 2009; current version published July 15, 2009. This work was supported by the National Institutes for Health through a Phase II STTR, subcontracted from Supercon, Inc..

X. T. Liu is with the Applied Superconductivity Center, National High Magnetic Field Laboratory (NHMFL), Florida State University, Tallahassee, FL 32310, USA (e-mail: liuxt@magnet.fsu.edu).

W. T. Nachtrab and T. Wong are with Supercon Inc., Shrewsbury, Massachusetts, USA.

J. Schwartz is with the Applied Superconductivity Center, National High Magnetic Field Laboratory (NHMFL), Florida State University, Tallahassee, FL 32310, USA. He is also with the Department of Mechanical Engineering, FAMU-FSU College of Engineering, Tallahassee, FL, USA.

Color versions of one or more of the figures in this paper are available online at http://ieeexplore.ieee.org.

Digital Object Identifier 10.1109/TASC.2009.2018497

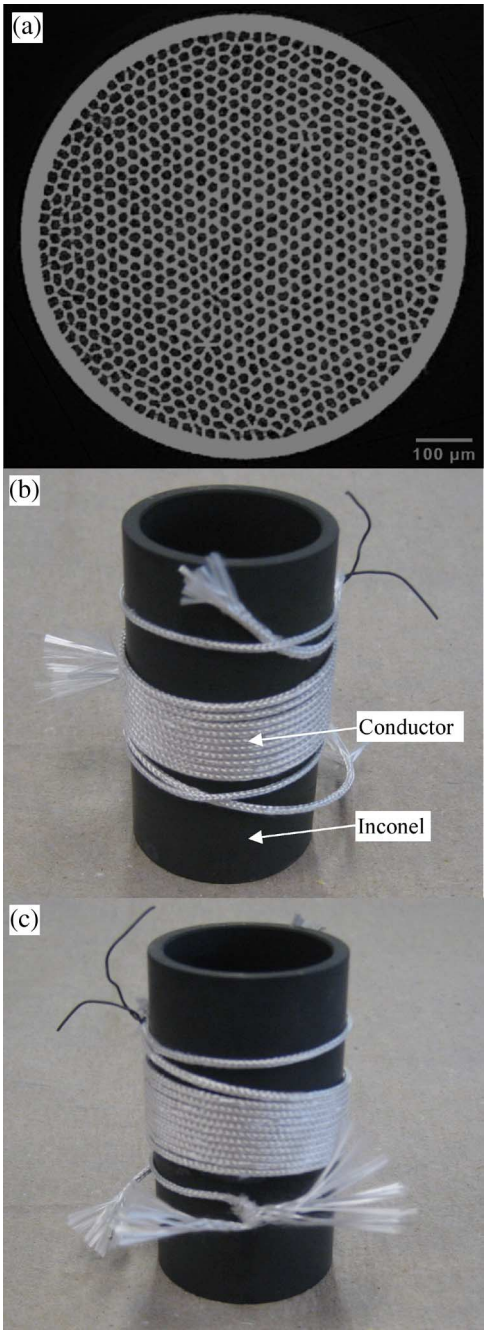

Fig. 1. (a) Cross section of a 0.787 mm diameter green wire, (b) a single-layer coil before heat treatment, and (c) the same single-layer coil after heat treatment.

The second heat treatment reheats the coil to 833°C at 80°C/h, holds for 48 h and then cools to room temperature at 80°C/h. This is a version of the split melt processing associated with the react-wind-sinter coil manufacturing approach [5], [7], [8]. With each coil heat treatment, six witness samples (three without insulation and three with insulation) are heat treated for comparison with coil performance.

After full heat treatment, the coil is electrically tested and then deconstructed into short samples for transport and magnetization measurements and microanalysis. For short samples, I_c measurements are made at 4.2 K, self-field using the standard four point method on 4 cm samples with a 1 μV/cm electric field criterion and a 18–20 mm voltage tap spacing. For coils, I_c is measured end-to-end (ETE) and every two turns in magnetic

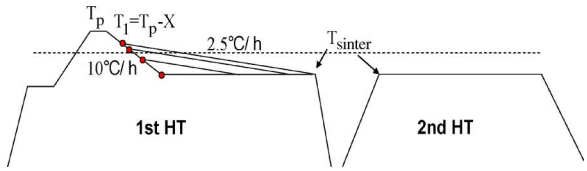

Fig. 2. Temperature-time schematic of the split-melt processing heat treatment profile used for short-sample and coil processing.

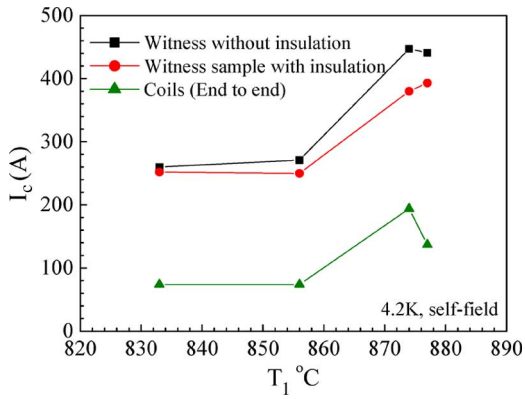

Fig. 3. Effect of T_1 on the I_c of coils and witness sample.

fields up to 5 T at 4.2 K. The superconducting transition is measured in a 100 G magnetic field in a SQUID magnetometer. Microstructures are examined using an SEM with EDS on a Zeiss 1540 EsB microscope. Each phase composition is an average of 5–10 measurements.

III. Results and Discussion

Leakage from the wires during heat treatment is one of the remaining challenges facing Bi2212 coil technology. In the coils studied here, some tendency towards leakage was observed but a number of coils were heat treated without any visible leakage resulting. In general, leakage tended to occur primarily during the first heat treatment, but not in the second heat treatment.

Fig. 3 shows I_c of coils and witness samples as a function of T_1. Here, the ETE I_c is shown for coils. In general, I_c decreases with decreasing T_1 for all sample types. I_cs of witness samples with insulation are consistently 10–15% lower than those heat treated without insulation. The coil performance versus T_1 shows the same tendency as the witness samples except for the coil processed at $T_1 = 877$°C which has slightly reduced I_c due to the existence of several visible leaks after full heat treatment. The ETE I_c of coils is consistently ~50% less than that of witness samples heat treated with insulation. For Bi2212, partial-melt processing, including the first heat treatment in the split-melt process used here, consists of heating the Bi2212 above its peritectic temperature, cooling quickly from the peak temperature to T_1 and then slow cooling during which Bi2212 phase is formed. Once T_1 is reached, the cooling rate is significantly slowed, so varying T_1 essentially varies the amount of time the superconductor is in the partial-melt state. Decreasing T_1 increases the effective overall cooling rate. When T_1 is low, the coil performance becomes relatively independent of T_1 which indicates that the initial cooling rate is most significant and that the effect of T_1 on coil performance is actually a cooling-rate effect. While lower performance is observed,

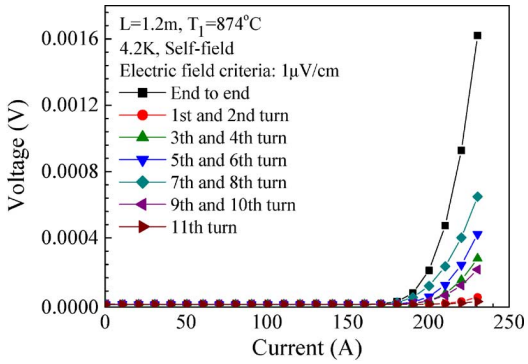

Fig. 4. Self-field V-I curves for a coil heat treated with $T_1 = 874°C$.

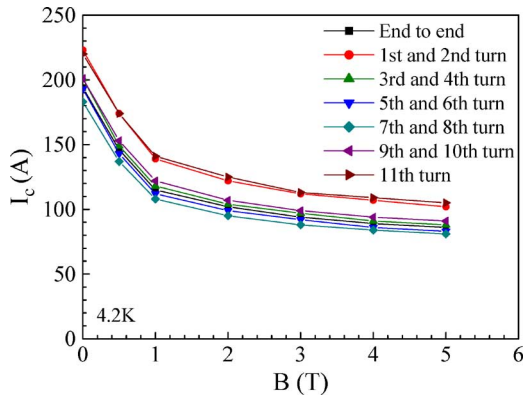

Fig. 5. I_c versus B for a coil heat treated with $T_1 = 874°C$.

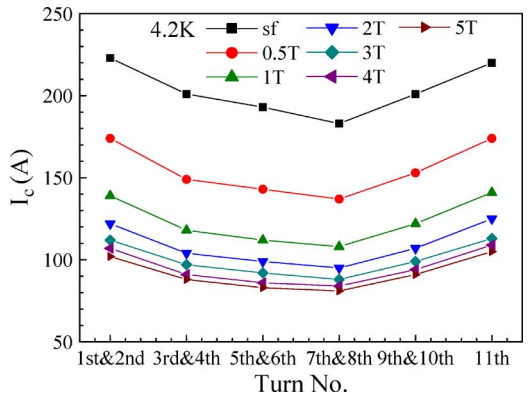

Fig. 6. I_c distribution as a function of magnetic field within a coil heat treated at $T_1 = 874°C$.

it is also important to note that reduced T_1 also reduces the occurrence of leakage during coil heat treatment.

Fig. 4 shows typical V-I curves for a coil, including the ETE measurement and measurements on every two turns. This coil was heat treated with $T_1 = 874°C$. Figs. 5 and 6 show the I_c of the same coil as a function of magnetic field and turn number, respectively. It is seen that the V-I curves fall into two groups; one is the end turns with higher I_c and the other is the middle turns with lower I_c. Compared to the ends, I_c of the middle turns is ~18% lower.

Fig. 7 shows the current distribution after the coils are deconstructed into 55 mm long short samples. Table I shows the differences in I_c ($\Delta I_c = I_{c,max} - I_{c,min}$ for a given coil) between short samples cut from the end and middle sections. It is seen that these cut short samples show the same tendency as the

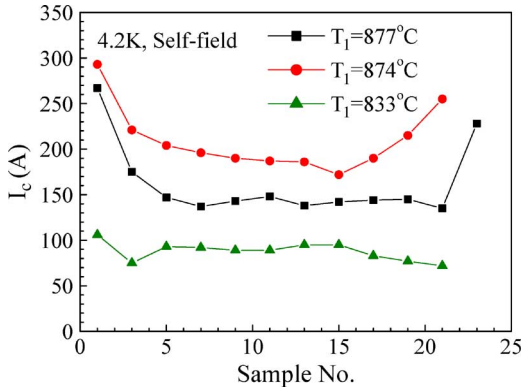

Fig. 7. I_c distribution of short samples deconstructed from coils heat treated at different T_1.

TABLE I
I_c COMPARISON FROM SAMPLES CUT FROM THE MIDDLE AND END SECTIONS OF COILS (ΔI_C IS DEFINED AS $I_{C,MAX} - I_{C,MIN}$)

T_1 (°C)	ΔI_c (A)	$\Delta I_c/I_{cmax}$ (%)
833	17	16
874	106	36
877	119	45

two-turn measurements seen in Figs. 4–6, with higher current in the end sections and lower current in the middle sections. For the coils processed at different T_1, however, the difference in I_c between end and middle sections decreases from 45% to 16% as T_1 decreases from 877°C to 833°C. In essence, as T_1 increases, I_c increases in the end turns significantly more than the middle turns.

Fig. 8 shows the superconductive transition of witness samples and short samples cut from end and middle sections of coils. For witness samples, there is no great difference in onset T_c due to T_1 variations but the connectivity decreases greatly when $T_1 = 833°C$. For short samples cut from coil sections, the superconductive transition curves are shallower than those of the witness samples and the superconductive transition curves of the samples cut from the middle sections are shallower than those cut from the end sections, especially when treated at higher T_1. This indicates that the short samples cut from coil sections, especially middle sections, have lower connectivity than the witness samples.

Fig. 9 shows the microstructures of witness samples and different coil sections after full heat treatment at different T_1. Each figure shows the microstructures of four samples: a witness sample without insulation (top left), a witness sample with insulation (top right), and short samples cut from an end section (bottom left) and a middle section (bottom right) of a coil. Also shown is the corresponding I_c for each sample at 4.2 K, self-field. Fig. 10 shows the microstructures in the center of wires after heat treatment (shown are the witness samples heat treated without insulation) at different T_1. Figs. 9 and 10 illustrate that, for the witness samples and coil sections heat treated at the higher T_1 (877°C and 874°C), there is no significant difference in the microstructures in the wire center.

For samples (both witness and coil sections) heat treated at higher T_1, large Bi2212 grains form and the interfilament bridging is well developed. At $T_1 = 833°C$, the Bi2212 grain size is small and the interfilament bridging is minimal;

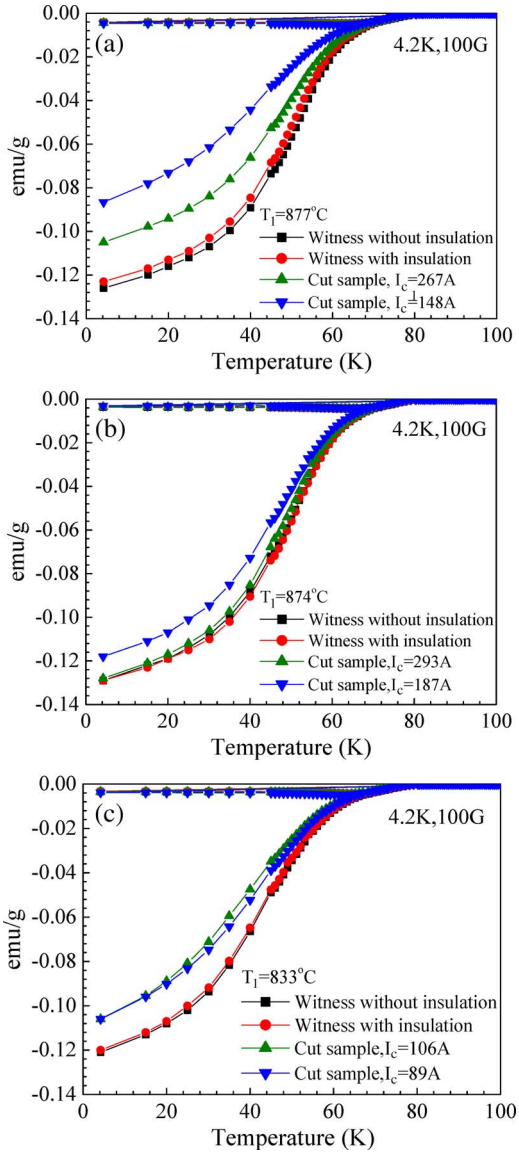

Fig. 8. Superconductive transition by magnetic measurements of witness samples and extracted coil samples heat treated with varying T_1. Here, two typical extracted coil samples with the highest I_c (end) and lowest I_c (middle) are shown.

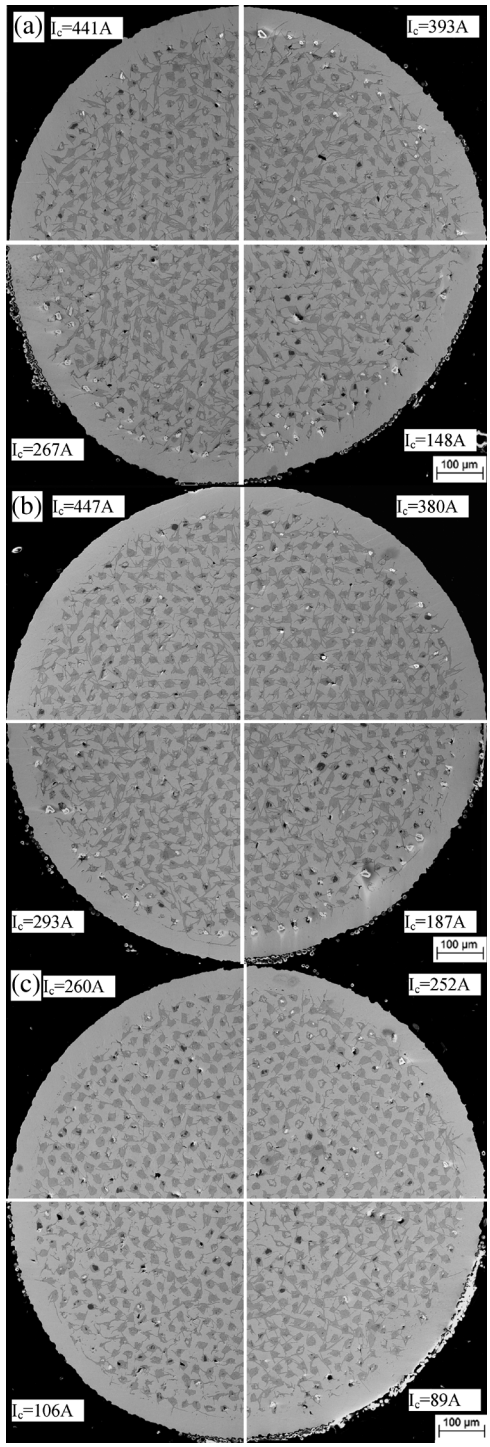

Fig. 9. Microstructure of witness samples and short samples cut from coil sections. Top left: witness sample without insulation; top right: witness sample with insulation; bottom left: short sample cut from a coil with the highest I_c; and bottom right: short sample cut from a coil with the lowest I_c). (a) $T_1 = 877°C$, (b) $T_1 = 874°C$, and (c) $T_1 = 833°C$. I_cs are shown with each image.

the filaments remain isolated after heat treatment. Decreasing T_1 corresponds to decreasing the duration in the partial-melt state due to the higher cooling rate for a longer period of time during solidification and growth. The faster cooling rate promotes Bi2212 grain nucleation and limits Bi2212 grain growth, resulting in smaller grain size than in samples with a slower cooling rate. Larger grains typically correspond to improved connectivity between grains [7]. Thus, the connectivity between Bi2212 grains decreases with decreasing T_1, which is consistent with the magnetic transition measurements seen in Fig. 8.

It is important to note that the microstructures of the outer filaments differ greatly between witness samples with and without insulation and short samples cut from different coil sections as shown in Fig. 9. For samples with insulation, more copper-free phase exists in the outer filaments compared to the witness samples without insulation. In samples cut from coil sections, especially short samples cut from the lower I_c middle sections, the amount of copper-free phase is increased and more filaments are lost compared to the witness samples. With decreasing T_1, the copper-free phases in the outer filaments decrease and the difference between witness samples and samples cut from coil sections also decreases. When T_1 decreases to 833°C there is no significant difference between witness samples and the samples cut from coil sections. These observations are consistent with the transport properties.

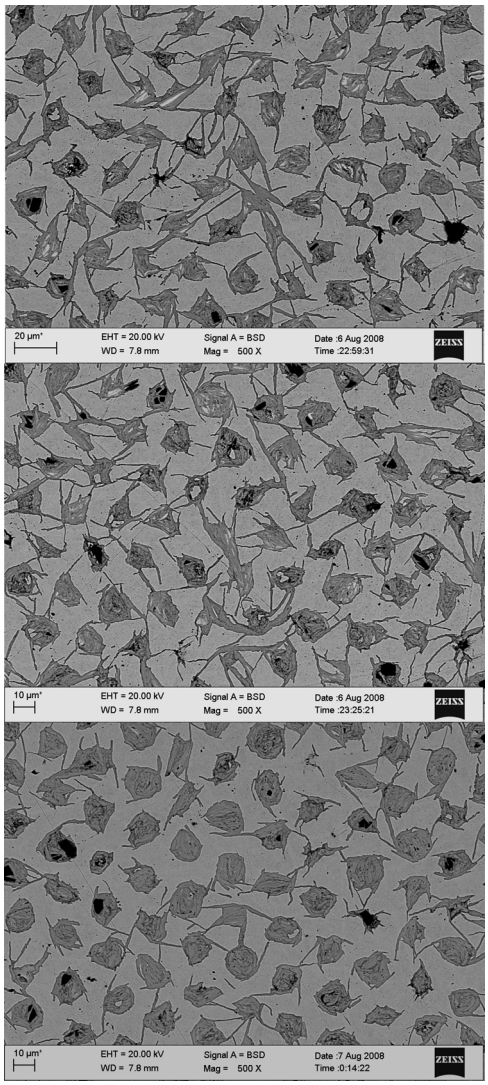

Fig. 10. Microstructure in the center of wires heat treated without insulation at different T_1 where (a) $T_1 = 877°C$, (b) $T_1 = 874°C$, and (c) $T_1 = 833°C$.

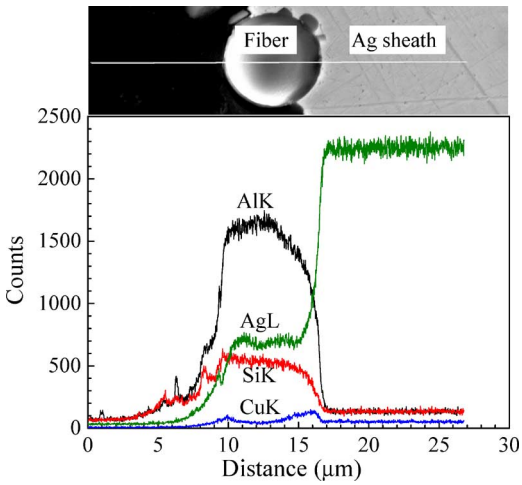

Fig. 11. Microstructure and EDS line scans of the Ag sheath and insulation fiber after full heat treatment.

Fig. 11 shows the reaction between the Ag sheath and insulation fibers and a corresponding EDS line scan analysis. After full heat treatment, Ag and Cu have reacted with the insulation. The Cu diffuses through the Ag sheath and interacts with the insulation, resulting in reduced copper content in the filaments, and in particular in the outer filaments. This results in a copper deficiency within the filaments and thus increased copper-free phase content in the outer filaments. Due to the tight contact between the conductor and insulation on the middle section of coils, Cu diffusion from filaments through the Ag sheath is accelerated, leading to increased copper-free phase content and lost filaments. As a result, the transport performance of the middle sections of the coils are decreased compared to those of the end sections.

IV. Conclusions

A series of single-layer coils and witness samples with and without insulation were heat treated. All heat treatments were identical with the exception of varying the temperature at which the cooling rate changes, T_1. Reduced T_1 is beneficial in that coil leakage is reduced, but reduced Bi2212 grain size and interfilament bridging result in reduced I_c.

The distribution of performance within the coils was studied and it was found that the end sections consistently have higher I_c. than middle sections of a coil. The difference in performance decreases as T_1 decreases.

Microstructural analysis of the wires and insulation shows that Ag and Cu react with the insulation fiber. In particular, Cu diffuses from filaments through the Ag to the insulation, resulting in decreased Cu content in the filaments and thus increased copper-free phase and filament loss due to leakage from the outer filaments.

Acknowledgment

The authors thank Dr. U. P. Trociewitz for many useful discussions.

References

[1] K. R. Marken, H. Miao, M. Meinesz, B. Czabaj, and S. Hong, "Progress in Bi-2212 wires for high magnetic field applications," *IEEE Trans. Appl. Supercond.*, vol. 16, no. 2, pp. 992–995, 2006.

[2] J. Schwartz, T. Effio, X. Liu, Q. V. Le, A. L. Mbaruku, H. J. Schneider-Muntau, T. Shen, H. Song, U. P. Trociewitz, X. Wang, and H. W. Weijers, "High field superconducting solenoids via high temperature superconductors," *IEEE Trans. Appl. Supercond.*, vol. 18, no. 2, pp. 70–81, 2008.

[3] T. Hase, Y. Murakami, S. Hayashi, Y. Kawate, T. Kiyoshi, H. Wada, S. Sairote, and R. Ogawa, "Development of Bi-2212 multifilamentary wire for NMR usage," *Physica C*, vol. 335, pp. 6–10, 2000.

[4] H. W. Weijers, U. P. Trociewitz, K. Marken, M. Meinesz, H. Miao, and J. Schwartz, "The generation of 25.05 T using a 5.11 T $Bi_2Sr_2CaCu_2O_x$ superconducting insert magnet," *Supercond. Sci. and Tech.*, vol. 17, pp. 636–644, 2004.

[5] X. T. Liu, T. M. Shen, U. P. Trociewitz, and J. Schwartz, "React-wind-sinter processing of high superconductor fraction $Bi_2Sr_2CaCu_2O_x/AgMg$ round wire," *IEEE Trans. Appl. Supercond.*, vol. 18, no. 2, pp. 1179–1183, 2008.

[6] S. L. Huang and D. Dew-Hughes, "Comprehensive investigation on microstructural and transport properties of electrophoretically deposited $Bi_2Sr_2CaCu_2O_{8+\delta}/silver$ composite tapes with various heat treatment conditions," *Physica C*, vol. 319, pp. 104–126, 1999.

[7] J. Schwartz and G. A. Merritt, "Proof-of-principle experiments for react-wind-sinter manufacturing of Bi2Sr2CaCu2O8+x magnets," *Supercond. Sci. and Tech.*, vol. 20, pp. L59–L62, 2007.

[8] T. M. Shen, X. T. Liu, U. P. Trociewitz, W. T. Nachtrab, T. Wong, and J. Schwartz, "Mechanical behavior of Bi2Sr2CaCu2Ox conductor using a split melt process for react-wind-sinter magnet fabrication," *IEEE Trans. Appl. Supercond.*, vol. 18, no. 2, pp. 520–524, 2008.

[9] R. Funahashi, I. Matsubara, K. Ueno, and H. Ishikawa, "Mechanism of $Bi_2Sr_2CaCu_2O_x/Ag$ tapes prepared using isothermal partial melting method," *Physica C*, vol. 311, pp. 107–121, 1999.